Collective magnetostatic modes on a one-dimensional array of ferromagnetic stripes

M. P. Kostylev,[1] A. A. Stashkevich,[2,*] and N. A. Sergeeva[1,2]
[1]*St. Petersburg Electrotechnical University, 197376 Saint-Petersburg, Russia*
[2]*LPMTM CNRS (UPR 9001), Université Paris 13, 93430 Villetaneuse, France*
(Received 14 August 2003; published 12 February 2004)

The peculiarities of collective magnetostatic modes on a one-dimensional array of ferromagnetic stripes have been studied. It has been shown that the frequency splitting, induced via dipole magnetostatic coupling in the oscillations of otherwise individual stripes, can achieve the values of the order of several GHz. This makes it easily observable by means of a standard Brillouin light spectrometer. To quantify the investigated effects, an analytical technique developed earlier for an isolated stripe has been extended to the case of a one-dimensional array of ferromagnetic stripes. The magnetization profiles of the stripes in the presence of strong coupling have been estimated numerically.

DOI: 10.1103/PhysRevB.69.064408 PACS number(s): 75.75.+a, 75.30.Ds, 75.50.−y

I. INTRODUCTION

The physics of nanopatterned magnetic structures has driven extensive research in recent years with both static and dynamic behavior being investigated. The applied aspect of these studies should not be underestimated either. A rapid increase of processor speeds in modern computers has led to the necessity of writing gigabits of information in a fraction of a second. This means that the magnetic system is excited at gigahertz rates and the inevitable generation of spin waves will strongly influence the response of magnetic recording media. In this respect, it is necessary to prevent the mutual influence of adjacent magnetic elements through inevitable coupling via the dynamic dipolar magnetic fields of individual elements. The key parameter governing such coupling is the spatial separation of the elements. To minimize the overall size of the structure, this separation must be kept as small as possible. On the other hand, if the elements are brought too close together, spurious *collective* magnetostatic modes will be excited through the thus-increased coupling. In the case of nanodots, where the fundamental magnetic state corresponds to a vortex configuration, this leads to a considerable mutual influence between the dots during the magnetization reversal,[1] as well as magnetostatic coupling[2] between the dynamic modes of individual vortices.[3] Similarly, in the case of nanowires of cylindrical cross section, both in theory[4] and in experiment,[5] collective modes due to the interplay between individual wires have been reported.

To study the basic properties of collective modes on periodic nanostructures we restricted our analysis to an ideal model object: a one-dimensional array of ferromagnetic stripes. Thus, simple and efficient numerical procedures can be developed backed by analytical expressions providing more physical insight.

The magnetostatic coupling between the individual resonances in a collective mode produces two effects: a redistribution of the dynamic magnetization on each element and a corresponding frequency shift. The Brillouin light scattering (BLS) technique has proved to be a very efficient method for directly measuring the dispersion characteristics of magnons on periodic structures.[6–14] Moreover, by recording the shape of a spectral line in Fourier space—i.e., in the K space of transferred wave vector—one can retrieve information on the distribution of magnetization on each element of the array.[6,9] Otherwise, it can be done directly, with more precision, by means of Kerr microscopy.[15,16]

Until lately, the problem of magnetostatic modes on one-dimensional ferromagnetic objects had no solution except one which is purely *numerical*.[8] It was generally accepted that the magnetic field at the edges of the film, to the first approximation, tends to zero.[17] In other words, the spins at the edges of the film are totally "pinned." In a recent paper[18] the authors proposed an *analytical* formalism. It expresses the modal distribution of the magnetic field across the width of a magnetic stripe, in a nonexchange approximation, as an eigenfunction of an integral equation. Thus the demagnetizing fields at the edges of the stripe are taken into account and effective pinning conditions introduced. We have extended this approach to the case of a periodic array of ferromagnetic stripes and have obtained the dispersion characteristics of the collective modes existing on such structures.

II. THEORY

Any coupling between individual stripes in an array is due to the long-range dipole-dipole interactions. Such coupling is most pronounced for the lowest width modes of a finite-width stripe which is, in most cases, of a dipole nature. That is why in order to calculate the dipolar coupling between the individual stripes we will extend the approach developed in Ref. 18, which is based on one-dimensional Green's functions $P(\xi,\xi')$. According to this approach, the dynamical magnetization $m(\xi)$ in a magnetostatic mode can be determined as an eigenfunction of the integral equation

$$\lambda m(\xi)=\int_{-1/2}^{1/2} d\xi' P(\xi,\xi')m(\xi'), \tag{1}$$

with

$$P(\xi,\xi')=\frac{1}{p}\ln\frac{(\xi-\xi')^4}{[p^2+(\xi-\xi')^2]^2},$$

$$\xi=x/w,\quad p=L/w.$$

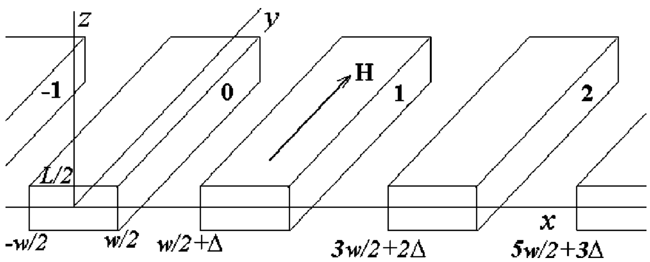

FIG. 1. Geometry of the structure. Stripe thickness is L, its width is w, and distance between neighboring stripes is Δ.

Here $P(\xi,\xi')$ is the Green's function calculated in the magnetostatic approximation and λ is the eigenvalue, corresponding to the eigenfunction $m(\xi)$. This expression has been obtained through averaging the general expression relating the magnetization to the dipolar magnetic field induced by it over the thickness of the film (i.e., over z). It will be shown below that the resultant purely dipolar modes are characterized by a quasicosinusoidal distribution of the dynamic magnetization across the width of a stripe, which makes a generalization of the dipole-exchange case rather straightforward.

This generalization is uncomplicated for the case of a magnetic field inside a stripe with number j created by a series of N parallel stripes (Fig. 1) arranged with dimensionless period $T=(1+\Delta/w)$:

$$\lambda m_j(\xi)=\sum_{j'=0}^{j'=N}\int_{-1/2}^{1/2}P(\xi,\xi'+(j'-j)T)\times m_{j'}[\xi'+(j'-j)T]d\xi', \tag{2a}$$

where ξ and ξ' are local coordinates within each individual stripe $(-1/2<\xi,\xi'<1/2)$ and Δ is the distance between the neighboring stripes. In the case of an infinite series of stripes a more symmetrical presentation is preferable:

$$\lambda m_j(\xi)=\sum_{j'=-\infty}^{j'=\infty}\int_{-1/2}^{1/2}P(\xi,\xi'+(j'-j)T)\times m_{j'}[\xi'+(j'-j)T]d\xi'. \tag{2b}$$

The system of coupled singular integral equations (2b) is too complex for an analytical solution to be found. In its general form it can only be analyzed numerically. To handle the computational problems arising from the nonanalytical behavior of the kernel in the vicinity of the point $\xi=\xi'$ we used the method proposed in Refs. 19 and 20. Here for the subtraction of the singularity we took advantage of the fact that the integral of the Green's function may be evaluated analytically over the range $-1/2<\xi<1/2$. To streamline the computational procedure we made use of the Nystrom method and the Gaussian quadrature.[20]

However, in some particular cases analytical solutions do exist. Let us consider one of them. As is well known,[21] the solution of a linear equation with periodic coefficients has the form

$$m_j(\xi)=\tilde{m}(\xi)\exp[ik(\xi+jT)], \tag{3}$$

where $\tilde{m}(\xi)$ is a periodic function with the period T,—i.e., $\tilde{m}(\xi+T)=\tilde{m}(\xi)$. The wave number k for the first Brillouin zone may vary within the range $0<k<\pi/2$. It should be noted that by considering Eq. (2b) in Fourier space it is easy to demonstrate that solution (3) really stands.

Inserting Eq. (3) into Eq. (2b) results in

$$\lambda\tilde{m}_j(\xi)=\sum_{j'=-\infty}^{j'=\infty}\int_{-1/2}^{1/2}P(\xi,\xi'+(j'-j)T)\times\exp\{ik[\xi'-\xi+(j'-j)T]\}\tilde{m}_j(\xi')d\xi'. \tag{4}$$

In the limit $2\pi/k\ll w$—i.e., when the spatial period of the collective mode is much greater than that of the wire array—we may assume

$$\exp\{ik[\xi'-\xi+(j'-j)T]\}\approx\exp[ik(j'-j)T]\equiv\exp[i(j'-j)\Delta\varphi], \tag{5}$$

where $\Delta\varphi$ represents the relative phase of the oscillations of two adjacent stripes. Furthermore, if the period of the structure is much greater than the width of the stripes—that is, $T\gg1$—from general considerations it is clear that effective coupling is only possible between two adjacent stripes. Therefore, on the right-hand side of Eq. (5) we may only keep three terms corresponding to $j-1$, j, $j+1$:

$$m_{j-1}(\xi)=\tilde{m}(\xi)\exp[i(-\Delta\varphi)],$$

$$m_j(\xi)=\tilde{m}(\xi),$$

$$m_{j+1}(\xi)=\tilde{m}(\xi)\exp(i\Delta\varphi),$$

in which case Eq. (4) reduces to

$$\lambda\tilde{m}(\xi)=\int_{-1/2}^{1/2}P(\xi,\xi'-T)\tilde{m}(\xi')\exp(-i\Delta\varphi)d\xi'+\int_{-1/2}^{1/2}P(\xi,\xi')\tilde{m}(\xi')d\xi'+\int_{-1/2}^{1/2}P(\xi,\xi'+T)\tilde{m}(\xi')\exp(i\Delta\varphi)d\xi', \tag{6}$$

where the first term corresponds to the contribution of the stripe $j-1$ and the last one to that of the stripe $j+1$.

Taking advantage of the symmetry of the problem one can arrive at the following relation describing the dispersion of the collective mode [see the Appendix, Eq. (A10)]:

$$-\lambda\int_{-l/2}^{1/2}\tilde{m}^2(\xi)d\xi+2\int_0^{1/2}\tilde{m}(\xi)d\xi\int_0^{1/2}[P(\xi,\xi')\pm P(-\xi,\xi')]\tilde{m}(\xi')d\xi'+2\int_0^{1/2}\cos\Delta\varphi\tilde{m}(\xi)d\xi\int_0^{1/2}[C(\xi,\xi')\pm C(-\xi,\xi')]\tilde{m}(\xi')d\xi'=0. \tag{7}$$

Here, the upper sign corresponds to the case of symmetric modes and the lower one to the case of antisymmetric modes. This equation relates λ, which is a function of ω, to the phase shift between the adjacent stripes $\Delta\varphi$ which describes the wave number of a collective mode. Now let us adopt an approximation according to which at long distances between stripes ($T \gg 1$) the function $\tilde{m}(\xi)$ that appears in Eq. (7) practically does not differ from one of the eigenfunctions of Eq. (1), $m_n^0(\xi)$, with corresponding eigenvalue λ_n^0. In other words, the dynamic-magnetization distributions across each individual stripe in the array are very close to that in an absolutely separated stripe; the last expression can be considerably simplified:

$$\delta\lambda_n = \frac{2\cos\Delta\varphi}{\int_{-l/2}^{l/2}[m_n^0(\xi)]^2 d\xi}\int_0^{1/2} m_n^0(\xi)d\xi \int_0^{1/2}[C(\xi,\xi') \pm C(-\xi,\xi')]m_n^0(\xi')d\xi', \tag{8}$$

where $\delta\lambda_n$ gives us an addition to the eigenfrequencies λ_n^0 of individual stripes, determined by Eq. (1), due to coupling.

Obviously, the particular case $\Delta\varphi = 0$, when all neighboring stripes are in phase, corresponds to the lower boundary of the first Brillouin zone, whereas $\Delta\varphi = \pi$, when the neighboring stripes are in antiphase, to its upper boundary. Therefore, the frequency width of the Brillouin zone, resulting from the splitting of the resonant modes of an individual stripe due to coupling, may be roughly estimated as

$$\Delta\omega_n = \omega_n(\Delta\varphi = \pi) - \omega_n(\Delta\varphi = 0) = \frac{\omega_M^2 \Delta\lambda_n}{16\pi\omega_n^0}\left(1 + \frac{\lambda_n^0}{2\pi}\right), \tag{9a}$$

where $\omega_M = 4\pi\gamma M_0$ and

$$(\omega_n^0)^2 = \omega_H(\omega_H + \omega_M) - \omega_M^2\left[\frac{\lambda_n^0}{4\pi} + \left(\frac{\lambda_n^0}{4\pi}\right)^2\right] \tag{9b}$$

is the eigenfrequency of resonance of an individual stripe,[18] $\omega_H = 4\pi\gamma H$, H is the static field applied along the stripes, γ is the gyromagnetic ratio, M_0 is the saturation magnetization, and

$$\Delta\lambda_n = \frac{4}{\int_{-l/2}^{l/2}[m_n^0(\xi)]^2 d\xi}\int_0^{1/2} m_n^0(\xi)d\xi \int_0^{1/2}[C(\xi,\xi') \pm C(-\xi,\xi')]m_n^0(\xi')d\xi'. \tag{9c}$$

III. DISCUSSION

To study the major properties of a system of coupled stripes we have chosen the case $N = 2$ [Eq. (2a)]—i.e., a *system of three* parallel stripes. From general considerations, it is clear that the spectrum will represent a set of frequency triplets. If the distance between the stripes tends to infinity, the stripes become entirely separated, which leads to a threefold degeneracy within each triplet. This is no longer the case for a finite interstripe spacing: the dipolar coupling between stripes removes the degeneracy. To quantify these effects, we have numerically solved Eq. (2a) for $N = 2$. Figure 2 shows the spectrum of coupled resonances—i.e., collective mode—of a system of three iron stripes 50 nm thick, 1 μ m wide, separated by 50 nm. The spectrum was calculated numerically from Eq. (2b). Solid circles show the resonance frequencies. For comparison, a segment of a solid vertical line shows the frequency position of the first Brillouin zone of the spectrum of the collective mode on an infinite array of such stripes (see Fig. 4).

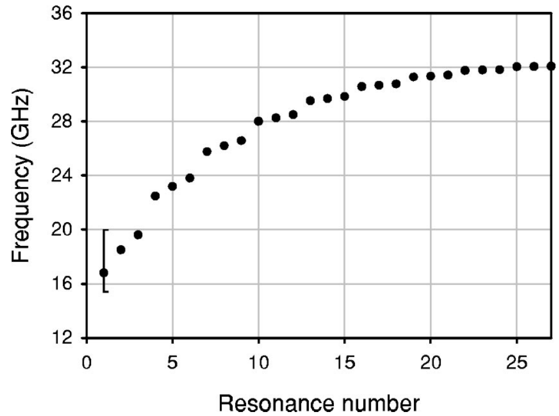

FIG. 2. Spectrum of collective modes in the system consisting of three parallel iron stripes of thickness 50 nm, having the same width of 1 μm, separated by a distance of 50 nm from each other. Saturation magnetization of the stripes is 21/(4π) kG; the static magnetic field applied along the stripes is 1 kOe.

The distributions of the dynamic magnetization for the lowest-frequency triplet are given in Fig. 3. As anticipated, the magnetization distributions of individual stripes, as well as the "dipolar" pinning conditions,[18] are markedly perturbed by the presence of the interstripe dipolar coupling. As a result, an appreciable frequency splitting $\Delta\omega_{spl}$ is introduced and the degeneracy is removed. Calculations show that the same is also valid for the higher triplets of resonances.

Obviously, the spatially quasihomogeneous dynamic demagnetizing field of the lowest resonance of an individual stripe is spread farther outside the stripe itself compared with higher resonances for which the field lines can be closed within the stripe itself. Therefore, for a finite distance between the stripes, the frequency of the lowest resonance of initially uncoupled stripes is affected most of all. This must produce the maximum frequency splitting in the lowest frequency triplet, which is clearly seen in Fig. 2.

Then, also numerically, by using Eq. (4) we calculated the dispersion $\omega(k)$ of the collective mode traveling across an *infinite array* of parallel coupled stripes of the same geometry. Figure 4 demonstrates the dispersion curve in the first Brillouin zone. It is obvious that the group velocity of the wave $V_g = \partial\omega(k)/\partial k$ depends on the zone width, which in its turn depends on the strength of the coupling. The group velocity is a very important parameter, because it determines the spatial damping of the wave and, therefore, the coupling distance in the real array where significant damping is always present. Another important parameter to be estimated is the frequency width $\Delta\omega_{Br}$ of the Brillouin zone: it determines the possibility of a direct observation of the coupling

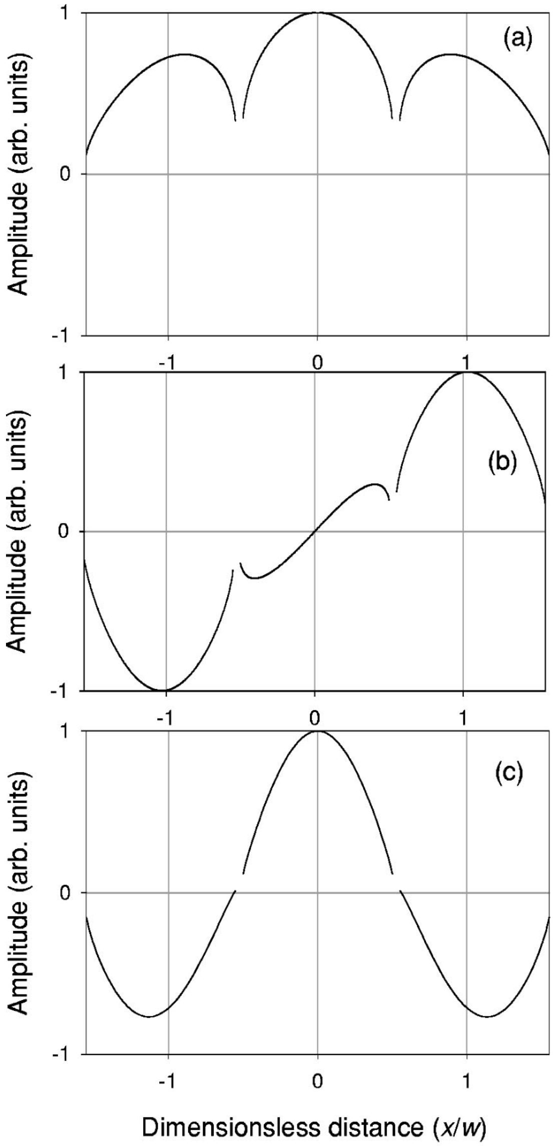

FIG. 3. Distribution of dynamic magnetization across a system of three parallel stripes for the three lowest resonant frequencies from Fig. 2. All the parameters of calculation are the same as in Fig. 2.

effect by using the BLS technique. In physical terms, the bandwidth of the first Brillouin zone corresponds to the frequency splitting in the first frequency triplet in Fig. 2. To compare the two quantities, in Fig. 2 the value of $\Delta\omega_{Br}$ is indicated with a segment of a solid vertical line. As is clearly seen, the two magnitudes differ only a little, being of the order of 3–4 GHz. Consequently, the frequency separation between two modes is about 1.5–2 GHz. The linewidth of the ferromagnetic resonance in iron is of the order of 100 Oe,[22] while the typical resolution of the Brillouin spectrometer is of the order of 300 MHz, indicating that the experimental measurement of the frequency splitting is quite feasible. As for recording the actual distribution of the magnetization across the stripes, it can be accomplished directly—for example, by means of Kerr microscopy[15,16]—or indirectly from the shape of a spectral

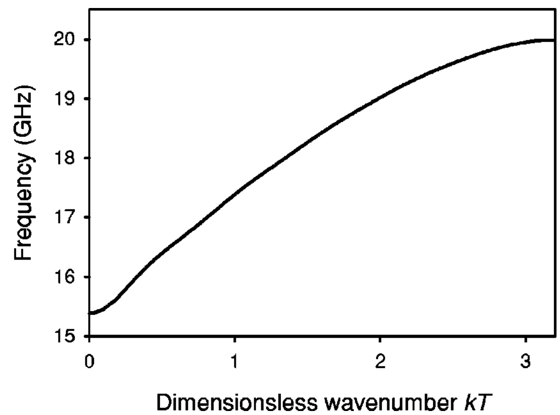

FIG. 4. Spectrum of the collective mode on an infinite array of iron stripes 50 nm thick and 1 μm wide. The stripes are separated by 50 nm. Saturation magnetization of the stripes is $21/(4\pi)$ kG; the static magnetic field applied along them is 1 kOe. The curve was calculated numerically from Eq. (4).

line of a Brillouin spectrometer in Fourier space.[6,9]

To better understand the behavior of the magnetostatic modes within the first Brillouin zone, another series of calculations has been carried out. The following considerations make it possible to substantially simplify the computational algorithm. As stated above, the lower boundary of the zone corresponds to a collective resonance in which the transverse distributions of dynamic magnetization across individual stripes are identical and in phase. This results in an equation as follows:

$$\lambda_{1L} m(\xi) = \int_{-1/2}^{1/2} m(\xi') \sum_{j=-\infty}^{j=\infty} P(\xi, \xi' + jT) d\xi', \quad (10a)$$

where $m(\xi)$ is the distribution of dynamic magnetization.

At the upper boundary of the zone, we also have a wave with identical distributions of magnetization on the stripes. However, the neighboring stripes are now in antiphase. This gives

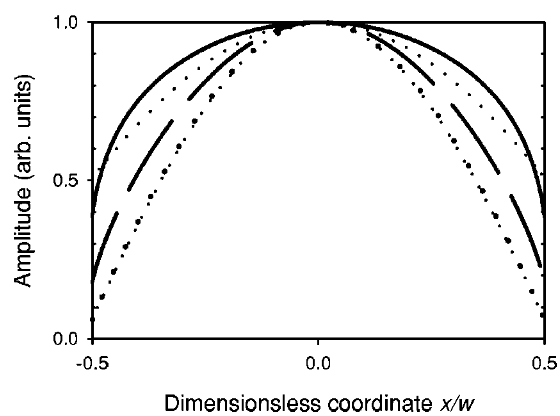

FIG. 5. Distributions of dynamic magnetization across an individual stripe in an infinite array. All the parameters of calculation are the same as in Fig. 4.

$$\lambda_{1U} m(\xi) = \int_{-1/2}^{1/2} m(\xi') \sum_{j=-\infty}^{j=\infty} (-1)^j P(\xi, \xi' + jT) d\xi'. \tag{10b}$$

For numerical calculations we used the usual method of consecutive approximations. Its efficiency for a kernel similar to that of Eqs. (10) was demonstrated recently.[23]

Given in Fig. 5 are the transverse distributions of the dynamic magnetization across individual stripes forming an infinite array. Thick solid and thick dotted lines demonstrate the rigorous solution and correspond to the lower and upper boundaries of the first Brillouin zone, respectively. They were calculated by numerically solving Eq. (4) both rigorously and approximately, introducing the effective local wave number (11). The thin dotted lines are the corresponding approximate solutions. Note that the approximate and rigorous solutions for the upper boundary practically coincide with graphical accuracy.

For comparison, the corresponding magnetization distribution on an isolated stripe numerically calculated from Eq. (1) is also placed in the figure, shown by a thick dashed line. The shape of the transverse distribution for an isolated stripe of the same width is shown by a dashed line. It is seen from the figure that the distributions of the dynamic magnetization, in particular the values at the stripe edge, differ appreciably at the upper and lower boundaries of the Brillouin zone. This can lead to a noticeable change in the shape of the spectral line of a Brillouin spectrometer in K space.

To study this effect we have approximated the solution of Eqs. (10) for the dynamic magnetization by a portion of a cosine function $m(\xi) = \cos(\chi\xi)$, $0 < \chi < \pi$. Then the eigenvalue of Eqs. (10) can be approximately found as the minimum of a function in χ:

$$\lambda_{1L(U)} = \min\left(\frac{\int_{-1/2}^{1/2}\int_{-1/2}^{1/2} d\xi d\xi' \cos(\chi\xi)\cos(\chi\xi') \sum_{j=-\infty}^{j=\infty} (\pm 1)^j P(\xi, \xi' + jT)}{\int_{-1/2}^{1/2}\int_{-1/2}^{1/2} d\xi d\xi' \cos(\chi\xi)\cos(\chi\xi')}, \chi \right). \tag{11}$$

Here the upper sign corresponds to the lower zone boundary and vice versa.

It should be noted that if the cosine function is approximated by its Taylor series, an analytical solution of the minimization problem (11) can be found. However, even when only two first terms of the Taylor expansion are retained the obtained expressions turn out to be cumbersome, making their applicability dubious. Direct numerical minimization of the functional in Eq. (11) is far more appropriate from the practical point of view.

In Fig. 5 the approximate solutions of Eq. (11) for $m(\xi)$ are shown by dotted lines. It is seen from the figure that $m(\xi)$ for the upper Brillouin zone boundary is very well approximated by a cosine function. The agreement with the rigorous solution for the lower boundary is worse, but we believe it still to be good enough to justify using the effective wave number χ to characterize the effective pinning at the stripe edges.

As the spacing between adjacent stripes is the crucial parameter governing interstripe dipolar coupling, we used it as a variable in the functions describing the behavior of the collective mode at the boundaries of the first Brillouin zone (see Fig. 6). Thus we have estimated the frequencies of the upper $\omega(\lambda_{1U})$ and lower $\omega(\lambda_{1L})$ boundaries of the Brillouin zone [Fig. 6(a)] and their difference $\Delta\omega = \omega(\lambda_{1U}) - \omega(\lambda_{1L})$ [Fig. 6(b)] as a function of the normalized interstripe distance Δ/w. To find $\omega(\lambda_{1U})$ and $\omega(\lambda_{1L})$ from the calculated values of λ_{1L} and λ_{1U} we used Eq. (9b).

It is seen from Fig. 6(b) that the bandwidth $\Delta\omega$ of the Brillouin zone, for metals like iron with high saturation magnetization [see Eq. (9a)], can exceed 5 GHz. In other words, it can be easily measured by means of the BLS technique.[6–14]

Note that the agreement between the eigenvalues obtained by directly numerically solving Eqs. (10) with those calculated from Eq. (11) is much better than that of the eigenfunctions. In particular, for the case of Fig. 6, the discrepancy between the values of $\Delta\omega$ calculated approximately making use of Eq. (11) and those rigorously calculated is less than 5%. Taking into account the variational stability of the function involved, this is not surprising.

Finally, in Fig. 6(c) the dependence of the effective wave numbers χ for the upper and lower zone boundaries is demonstrated. The calculations were made by using the approximate expression (11). In both Figs. 6(a) and 6(c) the dashed line corresponds to the upper boundary of the Brillouin zone and the dashed-dotted one to the lower boundary. All the parameters of calculation, except for the interstripe distance, are the same as in Fig. 4. The figure shows that the coupling increases the effective pinning at the upper zone boundary and diminishes it at the lower one. This result is qualitatively predictable. In the limit $\Delta/w \to 0$, the situation reduces to the case of the homogeneous precession in a nonstructured magnetic layer. At the same time, the upper zone boundary for $\Delta/w \to 0$ corresponds to a continuous magnetostatic wave with wave number π/w.

IV. CONCLUSION

When considering the problem of the magnetostatic oscillations on an array of magnetic elements one should take into account the dipolar interstripe coupling which leads to the formation of collective magnetostatic modes. We have investigated its role for the particular case of one-dimensional array of ferromagnetic stripes. As in any periodic structure,

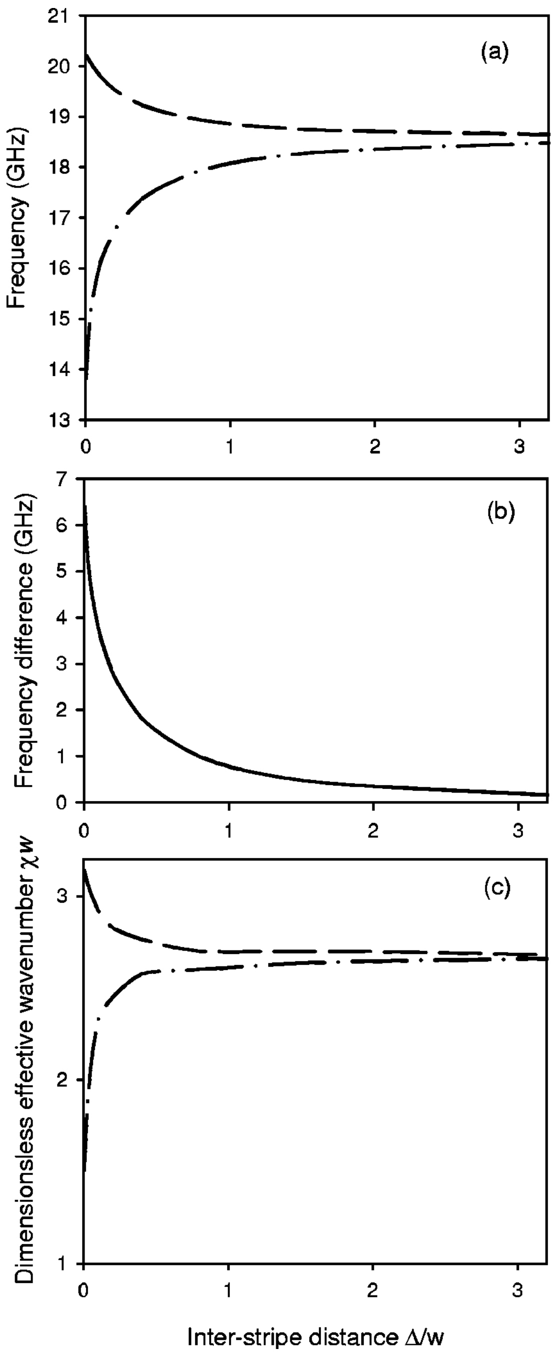

FIG. 6. (a) Eigenfrequencies of the collective mode vs the distance between the neighboring stripes in an infinite array of parallel stripes. (b) Difference of frequencies in (a). (c) Effective "local" wave number, describing the shape of the distribution of dynamic magnetization across an individual stripe of the array.

the collective modes in such array are characterized by a periodic dispersion curve comprised of Brillouin zones. Numerical simulations for the case of an array of iron stripes 50 nm thick, 1 μm wide, and separated by 50 nm show that the frequency band, corresponding to the first Brillouin zone, amounts to 4.5 GHz. This makes it easily observable by means of a standard Brillouin spectrometer.

To quantify the investigated effects, the analytical technique, developed earlier for an isolated stripe,[18] has been extended to the case of a one-dimensional array of ferromagnetic stripes. The profiles of magnetization on the stripes in the presence of strong coupling have been estimated numerically.

ACKNOWLEDGMENTS

This work was supported by the ACI "NANODYNE." One of us (M.K.) acknowledges the University Paris 13, whereas N.S. acknowledges the French Ministry for Foreign Affairs for support. The work was also supported in part by the Russian Foundation for Basic Research (Grant No. 02-02-16485) and by the Russian Ministry of Education (Grant No. 1292).

APPENDIX

Let us consider the sum of the first and the last term in Eq. (6) denoting it $W(\xi)$:

$$\begin{aligned} W(\xi) &= \int_{-1/2}^{1/2} [P(\xi,\xi'-T)\exp(-i\Delta\varphi) + P(\xi,\xi'+T) \\ &\quad \times \exp(i\Delta\varphi)]\tilde{m}(\xi')d\xi' \\ &= \cos\Delta\varphi \int_{T-1/2}^{T+1/2} C(\xi,\xi')\tilde{m}(\xi')d\xi' \\ &\quad - i\sin\Delta\varphi \int_{T-1/2}^{T+1/2} S(\xi,\xi')\tilde{m}(\xi')d\xi', \end{aligned} \tag{A1}$$

with

$$C(\xi,\xi') = \frac{1}{p}\ln\frac{(\xi-\xi'+T)^4(\xi-\xi'-T)^4}{[p^2+(\xi-\xi'+T)^2]^2[p^2+(\xi-\xi'-T)^2]^2},$$

$$S(\xi,\xi') = \frac{1}{p}\ln\frac{(\xi-\xi'+T)^4[p^2+(\xi-\xi'-T)^2]^2}{(\xi-\xi'-T)^4[p^2+(\xi-\xi'+T)^2]^2}. \tag{A1a}$$

The final expression will depend on the symmetry of the mode of magnetization $\tilde{m}(\xi)$.

In the case of a symmetric mode

$$\tilde{m}(-\xi') = \tilde{m}(\xi'). \tag{A2}$$

Taking the symmetry of the mode and the symmetry of the auxiliary function into account simultaneously,

$$S(-\xi,-\xi') = -S(\xi,\xi'), \tag{A3}$$

it is easy to show that

$$\int_{-1/2}^{1/2} \tilde{m}(\xi)\xi \int_{-1/2}^{1/2} S(\xi,\xi')\tilde{m}(\xi')d\xi' = 0. \tag{A4}$$

Similar calculations based on the symmetry of the

$$C(-\xi,-\xi') = C(\xi,\xi') \tag{A5}$$

lead to

$$\int_{-1/2}^{1/2}\tilde{m}(\xi)d\xi\int_{-1/2}^{1/2}C(\xi,\xi')\tilde{m}(\xi')d\xi' = \int_{-1/2}^{1/2}\tilde{m}(\xi)d\xi\int_{0}^{1/2}[C(\xi,\xi')+C(-\xi,\xi')]\tilde{m}(\xi')d\xi'$$
$$= 2\int_{0}^{1/2}\tilde{m}(\xi)d\xi\int_{0}^{1/2}[C(-\xi,\xi')+C(\xi,\xi')]\tilde{m}(\xi')d\xi'. \tag{A6}$$

In the case of an antisymmetric mode,

$$\tilde{m}(-\xi') = -\tilde{m}(\xi'), \tag{A7}$$

and application of Eqs. (A3) and (A7) describing the symmetry leads to the following expressions. As in the previous case,

$$\int_{-1/2}^{1/2}\tilde{m}(\xi)d\xi\int_{-1/2}^{1/2}S(\xi,\xi')\tilde{m}(\xi')d\xi' = 0. \tag{A8}$$

For the second integral we obtain

$$\int_{-1/2}^{1/2}\tilde{m}(\xi)d\xi\int_{-1/2}^{1/2}C(\xi,\xi')\tilde{m}(\xi')d\xi' = 2\int_{0}^{1/2}\tilde{m}(\xi)d\xi\int_{0}^{1/2}[C(\xi,\xi')-C(-\xi,\xi')]\tilde{m}(\xi')d\xi'. \tag{A9}$$

Inserting Eqs. (A4), (A6), (A8), and (A9) into Eq. (1) we arrive at the following dispersion equation for collective modes:

$$-\lambda\int_{-1/2}^{1/2}\tilde{m}^2(\xi)d\xi + 2\int_{0}^{1/2}\tilde{m}(\xi)d\xi\int_{0}^{1/2}[P(\xi,\xi')\pm P(-\xi,\xi')]\tilde{m}(\xi')d\xi'$$
$$+2\int_{0}^{1/2}\cos\Delta\varphi\,\tilde{m}(\xi)d\xi\int_{0}^{1/2}[C(\xi,\xi')\pm C(-\xi,\xi')]\tilde{m}(\xi')d\xi' = 0. \tag{A10}$$

*Electronic address: as@lpmtm.univ-paris13.fr.

[1] J. Shibata, K. Shigeto, and Y. Otani, Phys. Rev. B **67**, 224404 (2003).
[2] V. Novosad, M. Grimsditch, K. Yu. Guslienko, P. Vavassori, Y. Otani, and S. D. Bader, Phys. Rev. B **66**, 052407 (2002).
[3] V. Novosad, K. Yu. Guslienko, H. Shima, Y. Otani, S. G. Kim, K. Fukamichi, N. Kikuchi, O. Kitakami, and Y. Shimada, Phys. Rev. B **65**, 060402(R) (2002).
[4] R. Arias and D. L. Mills, Phys. Rev. B **67**, 094423 (2003).
[5] Z. K. Wang, M. H. Kuok, S. C. Ng, D. J. Lockwood, M. G. Cottam, K. Nielsch, R. B. Wehrspohn, and U. Gôsele, Phys. Rev. Lett. **89**, 027201 (2002).
[6] J. Jorzick, S. O. Demokritov, C. Mathieu, B. Hillebrands, B. Bartenlian, C. Chappert, F. Rousseaux, and A. N. Slavin, Phys. Rev. B **60**, 15 194 (1999).
[7] S. M. Chérif, Y. Roussigné, and P. Moch, Phys. Rev. B **59**, 9482 (1999).
[8] Y. Roussigné, S. M. Chérif, C. Dugautier, and P. Moch, Phys. Rev. B **63**, 134429 (2001).
[9] S. O. Demokritov, B. Hillebrands, and A. N. Slavin, Phys. Rep. **348**, 442 (2001).
[10] J. Jorzick, S. O. Demokritov, and B. Hillebrands, J. Appl. Phys. **89**, 7091 (2001).
[11] M. Grimsditch, I. Guedes, P. Vavassori, V. Metlushko, B. Ilic, P. Neuzil, and R. Kumar, J. Appl. Phys. **89**, 7096 (2001).
[12] J. Jorzick, S. O. Demokritov, B. Hillebrands, M. Bailleul, C. Fermon, K. Y. Guslienko, A. N. Slavin, D. V. Berkov, and N. L. Gorn, Phys. Rev. Lett. **88**, 047204 (2002).
[13] J. Jorzick, C. Krämer, S. O. Demokritov, B. Hillebrands, E. Sondergard, M. Bailleul, C. Fermon, U. Memmert A. N. Müller, A. Kounga, U. Hartmann, and E. Tsymbal, J. Magn. Magn. Mater. **226**, 1835 (2001).
[14] G. Gubbiotti, P. Candeloro, L. Businaro, E. Di Fabrizio, A. Gerardino, R. Ziveri, M. Conti, and G. Carlotti, J. Appl. Phys. **93**, 7595 (2003).
[15] J. P. Park, P. Eames, D. M. Engebretson, J. Berezovsky, and P. A. Crowell, Phys. Rev. Lett. **89**, 277201 (2002).
[16] J. P. Park, P. Eames, D. M. Engebretson, J. Berezovsky, and P. A. Crowell, Phys. Rev. B **67**, 020403(R) (2003).
[17] T. W. O'Keeffe and R. W. Patterson, J. Appl. Phys. **49**, 4886 (1978).
[18] K. Yu. Guslienko, S. O. Demokritov, B. Hillebrands, and A. N. Slavin, Phys. Rev. B **66**, 132402 (2002).
[19] H. Hochstadt, *Integral Equations* (Wiley, New York, 1975).
[20] W. H. Press, S. A. Teulkovsky, W. T. Vetterling, and B. P. Flannery, *Numerical Recipes in C* (Cambridge University Press, Cambridge, England, 1992).
[21] L. D. Landau and E. M. Lifshitz, *Mechanics*, Vol. 1 of *Course of Theoretical Physics* (Pergamon Press, New York, 1959).
[22] A. G. Gurevich and G. A. Melkov, *Magnetization Oscillations and Waves* (CRC Press, New York, 1996).
[23] C. Bayer, S. O. Demokritov, B. Hillebrands, A. N. Slavin, and M. P. Kostylev (unpublished).